Australian Seismological Reference Model (AuSREM): Crustal Component

M. Salmon, B.L.N. Kennett & E. Saygin

Research School of Earth Sciences, The Australian National University, Canberra ACT 0200*, Australia*

ABSTRACT

Although Australia has been the subject of a wide range of seismological studies, these have concentrated on specific features of the continent at crustal scales and on the broad scale features in the mantle. The Australian Seismological Reference Model (AuSREM) is designed to bring together the existing information, and provide a synthesis in the form of a 3-D model that can provide the basis for future refinement from more detailed studies. Extensive studies in the last few decades provide good coverage for much of the continent, and the crustal model builds on the various data sources to produce a representative model that captures the major features of the continental structure and provides a basis for a broad range of further studies. The model is grid based with a 0.5° sampling in latitude and longitude, and is designed to be fully interpolable, so that properties can be extracted at any point. The crustal structure is built from 5-layer representations of refraction and receiver function studies and tomographic information. The AuSREM crustal model is available at 1 km intervals.

The crustal component makes use of prior compilations of sediment thicknesses, with cross checks against recent reflection profiling, and provides P and S wavespeed distributions through the crust. The primary information for P wavespeed comes from refraction profiles, for S wavespeed from receiver function studies. We are also able to use the results of ambient noise tomography to link the point observations into national coverage. Density values are derived using results from gravity interpretations with an empirical relation between P wavespeed and density. AuSREM is able to build on a new map of depth to Moho, which has been created using all available information including Moho picks from over 12,000 km of full crustal profiling across the continent.

The crustal component of AuSREM provides a representative model that should be useful for modelling of seismic wave propagation and calculation of crustal corrections for tomography. Other applications include gravity studies and dynamic topography at the continental scale.

Key words: Australia, Crust, Body Waves, Surface Waves, Refraction, Receiver Functions

1 INTRODUCTION

The Australian Seismological Reference Model (AuSREM) is designed to capture the wide range of seismological information generated over the last few decades on the structure beneath the Australian region exploiting both natural and man-made sources. The objective of AuSREM is to provide a representation of the 3-D structure beneath Australia and its environs in a form that summarises existing knowledge and provides a basis for future refinement from more detailed studies. The aim is

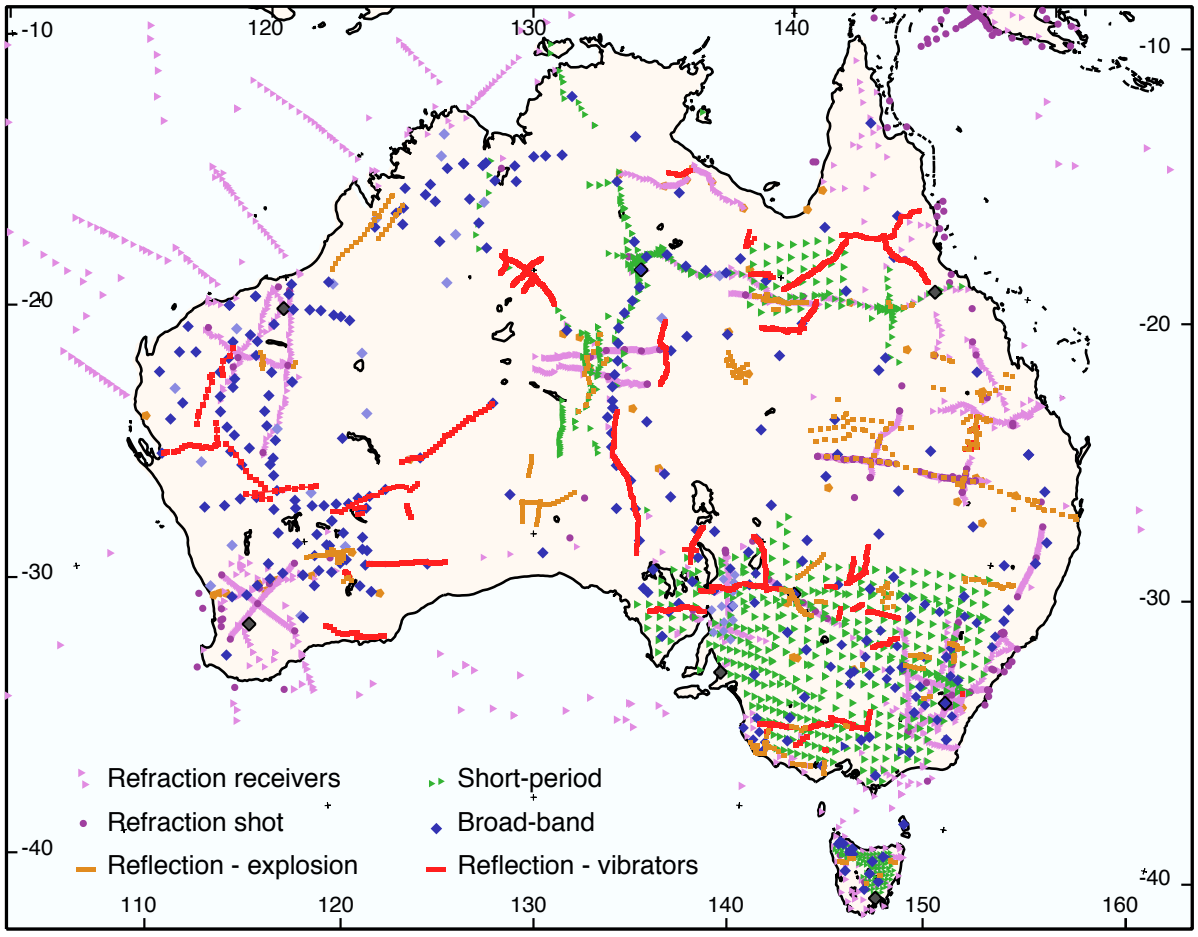

Figure 1. Location of seismological studies across Australia to mid 2012. Active studies: refraction surveys (purple) and shotpoints (circles), reflection lines (orange - explosive sources, red - vibrator sources) and passive studies: broad-band recording stations (diamonds) and short-period stations (triangles), as indicated on the key.

not to attempt to produce a definitive model, but rather to capture the major features of the continental structure in a way that will allow testing against future results. A general description of the construction of AuSREM and its implications is given by Kennett & Salmon (2012). A detailed discussion of the construction of the mantle component of AuSREM is to be found in Kennett et al. (2012).

Potential applications of AuSREM include delineation of major structural features and improved earthquake locations, both within Australia and at the immediate plate boundaries by using better representations of crustal and mantle structure. The reference model has been built using Australian specific information of varying vintage and quality which have been brought together in a unified framework. Improved knowledge of crustal structure will be of considerable value in work on seismic tomography, since the influence of crustal structure is significant for much of the frequency band used in surface wave tomography to study the lithospheric mantle and the asthenosphere beneath. The crustal model will also provide a useful starting point for delay time tomography.

An extensive program of investigation of Australian structure was instigated in the 1960's with short-offset reflection and later refraction studies carried out by the then Bureau of Mineral Resources (now Geoscience Australia). This program of active-source seismology has continued with over 12 500 km of full-crustal reflection profiles collected across the continent up to 2012. A complementary range of studies has been carried out using recordings of regional and teleseismic earthquakes using portable seismic recorders (see, e.g., Kennett 2003). Coverage of the whole continent has been achieved with portable broad-band stations, and higher density studies using portable recorders provide good coverage in the southeast. Additional permanent seismic stations have been installed in recent years. All of the passive seismic studies have continuous recording of ground motion and this data has been exploited using the recently developed techniques of ambient noise tomography (Saygin & Kennett 2010, 2012; Young et al. 2011) The coverage of the whole continent is relatively good (Figure 1) even though there are a number of prominent holes as a result of complex access and logistics, particularly in desert areas. The result is that the

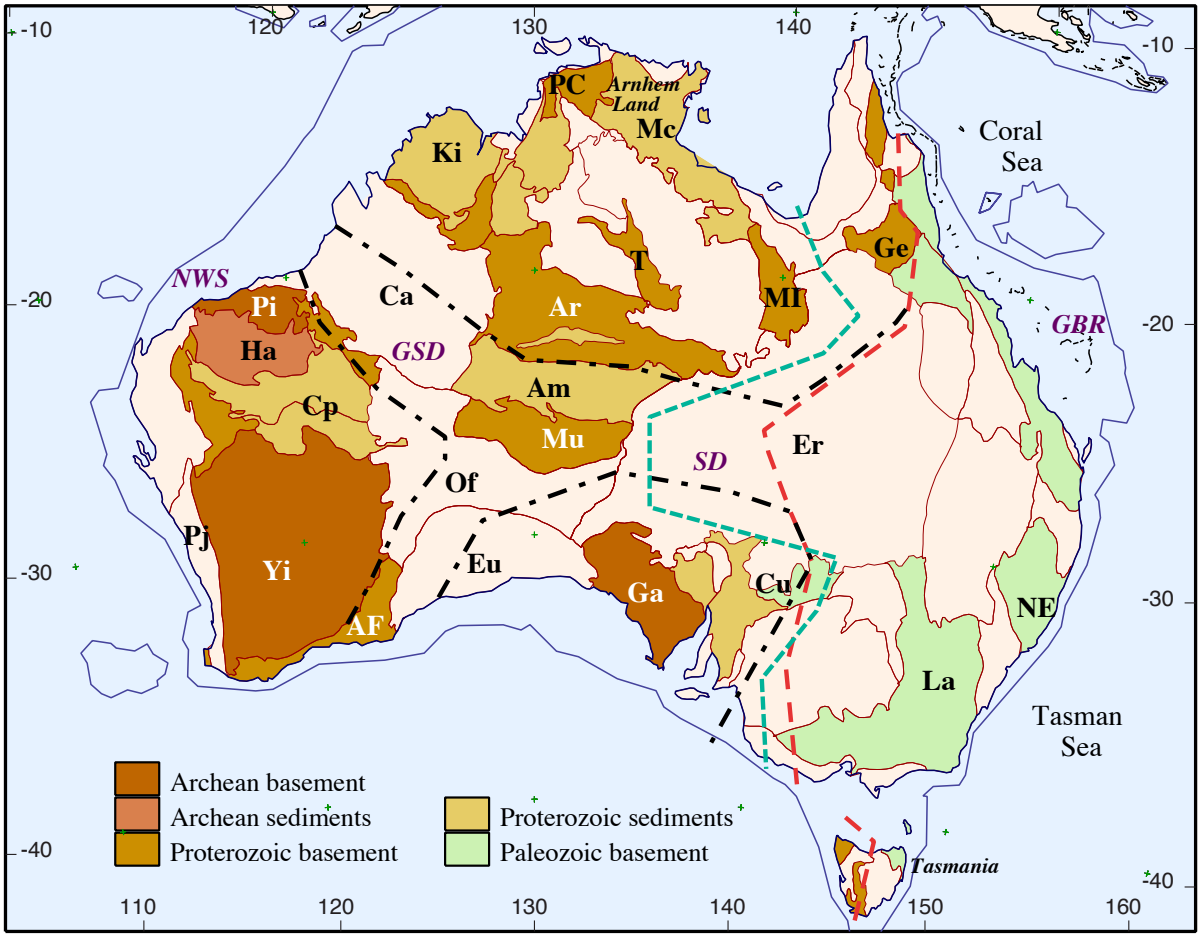

Figure 2. Simplified representation of the main tectonic features of Australia. The outline of the major cratons are marked by chain-dotted lines. The Tasman line in red is based on the reinterpretation by Direen & Crawford (2003). The cyan dashed line indicates the eastern boundary of the main block of thickened crust (after Kennett et al., 2011) Key to marked features: AF - Albany-Fraser belt, Ar - Arunta Block, Am - Amadeus basin, Ca - Canning basin, Cp - Capricorn Orogen, Cu - Curnamona craton, Er - Eromanga basin, Eu - Eucla basin, Ga - Gawler craton, Ge - Georgetown inlier, Ha - Hamersley basin, Ki - Kimberley Block, La - Lachlan Orogen, Mc - MacArthur basin, MI - Mt Isa Block, Mu - Musgrave Block, NE - New England Orogen, Of - Officer basin, PC Pine Creek Inlier, Pi - Pilbara craton, Pj - Pinjarra Orogen, T - Tennant Creek Block, Yi - Yilgarn craton, *NWS* - Northwest Shelf, *GBR* - Great Barrier Reef, *SD* - Simpson Desert, *GSD* - Great Sandy Desert.

broad features of the continent are well represented, such as the zone of generally thickened crust in central Australia, but the finer scales such details of sutures between the cratonic elements cannot be resolved.

For the crust the major sources of information are the seismic refraction experiments, supplemented by receiver function studies and the wavespeed distribution derived from ambient noise tomography for the whole continent. The reflection profiles provide an important source of information on crustal architecture and crustal discontinuities, and have played a major role in the recent development of a revised Moho depth model for the entire continent (Kennett et al. 2011).

1.1 Tectonic background

Rocks exposed at the surface in Australia span much of the Earth's geological history. The Archaean regions include rocks older than 3700 Ma in Western Australia and 3100 Ma in the Gawler Craton of South Australia. The oldest zircon crystals yet found on the Earth, dating back to 4400 Ma, occur in Proterozoic conglomerates within the northern Yilgarn Craton of Western Australia. In contrast, recent volcanic activity in both northeast and southeast Australia has left distinct volcanic edifices, with the latest eruptions in the southeast at about 4000 BCE.

Around 80% of Australia is covered by extensive Mesozoic and younger sedimentary rocks and regolith (Figure 2). These cover rocks indicate the general tectonic stability of much of the continent from Mesozoic times to the Present. The underlying Australian continental crust was accreted in three major supercontinent cycles, each comprising about one third of the continental area from the Archaean cratons in the west to Phanerozoic provinces in the east. Disparate Archaean crustal elements were assembled into three major cratonic zones in the Proterozoic. The West Australian, the North Australian, and the

Table 1. Representation of crustal structure at data points

Layer	h [km]	V_p [km/s]	V_s [km/s]	V_p/V_s
Sediments	0.0 - 2.0	1.0 - 4.3	0.5 - 1.5	2.00 - 3.00
Basement	0.0 - 3.0	2.8 - 5.4	1.7 - 2.7	1.65 - 2.00
Upper crust	5.0 - 20.0	4.8 - 6.8	2.9 - 3.9	1.65 - 1.80
Middle crust	5.0 - 20.0	5.6 -7.5	3.4 - 4.4	1.65 - 1.80
Lower crust	0.0 - 15.0	6.1 - 7.8	3.7 - 4.7	1.65 - 1.80

South Australian elements were formed by ~1830 Ma, and these cratonic elements were joined to the Rodinian supercontinent by 1300–1100 Ma (e.g. Betts et al. 2002; Cawood & Korsch 2008). Across northern Australia, large areas of mostly Proterozoic metasedimentary rocks occur in the Kimberly, Pine Creek, Macarthur and Mt Isa areas. These basins were filled with vast sandsheets during a time when the Earth's land surface was devoid of the stabilising influence of life, and have become the containers for major base metal and uranium mineral systems.

The fold belt structures of the Phanerozoic Tasman belt comprise the eastern third of Australia, which was accreted onto the eastern margin of the Precambrian cratons in the period from 500-300 Ma (e.g., Collins & Vernon 1992). The break up of Gondwana, through a series of rifting events from about 160 Ma, resulted in the formation of the passive margins around Australia, with the formation of the Coral and Tasman seas in the east, the Southern Ocean in the south and the Indian Ocean in the west (e.g. Huston et al. 2012). These rift events created the accommodation space for the Mesozoic sedimentary basins that host most of Australia's hydrocarbon resources.

There has been significant subsequent volcanism; in the Mesozoic, Australia was the continental margin of the subducting Pacific Plate and subsequently a chain of hot-spot related volcanism has developed through eastern Australia. The eastern margin of Australia has been influenced by sea-floor spreading in the Tasman Sea from ~80 Ma and back-arc spreading in the Coral Sea.

The eastern seaboard, including Tasmania, is a patchwork of Palaeozoic metamorphic, sedimentary and igneous rocks. These rocks are revealed, as highlands, due to the rift-flank uplift generated by opening of the Tasman and Coral seas (e.g., van de Beek et al., 1999). The Flinders Ranges, a Y-shaped region of uplifted Neoproterozoic sedimentary rocks in South Australia, attest to the influence of regional compression across the Australian Plate (Sandiford, 2003).

1.2 The AuSREM crustal model

The AuSREM model is grid based with 0.5 degree sampling in both latitude and longitude. The AuSREM crustal grid extends from 100°E to 160°E and from 10°S to 45°S. At each grid point the properties beneath are defined in terms of the depths of major boundaries such as the base of the sediments and the Moho, and the seismic P and S wavespeeds and density as a function of depth. The model is designed for interpolation, so that properties can be extracted at any point. AuSREM is built from Australian specific information rather than employing analogies with other parts of the world. In a number of the subsequent figures we employ $0.5^\circ \times 0.5^\circ$ pixels so that the effective resolution can be judged, but the AuSREM model itself is not cellular.

For the crust, much of the control from refracted waves is on the P wavespeed, and then S wavespeeds and density have to be inferred using other information. Receiver function inversion on the other hand provides S wavespeeds and particularly discontinuity depths, together with some controls on the ratio between P and S wavespeeds (e.g. Clitheroe et al., 2000). We have built up a database of well constrained results using different types of seismic data and gravity interpretations to aid with the extraction of the secondary variables. We use a 5-layered structure in the crust at each data point (see Table 1), with linear gradients in properties between the boundaries. This simple form provides considerable flexibility and has been widely used in seismic receiver function studies (e.g. Shibutani et al. 1996; Clitheroe et al. 2000; Reading et al. 2007, 2012). Summary values are extracted from the model across the entire grid at 5 km depth intervals.

We are able to draw on the recent compilation by Kennett et al. (2011) for the description of Moho depth. This model builds on the entire suite of available data from refraction, reflection and receiver function studies. The inclusion of Moho picks at 20–40 km intervals taken from extensive full-crustal reflection profiling has been particularly valuable in the construction of the Moho map. Previously isolated seismic stations can now be linked, and also cross-checks provided on results from other methods. In general, the consistency between techniques is very high and in most places the variation in crustal thickness estimates are less than 3 km.

The thickest crust (more than 50 km thick) is mapped beneath the eastern highlands, central Australia and the Mt Isa region. The crust thins towards the continental edge, although it is still over 35 km thick in regions of the North West Shelf. The thinnest crust on the mainland is around 30 km or less in the northeast part of South Australia; a region with coincident high heat-flow anomalies.

Table 2. Table of Data sources: RF - receiver functions, HRF - higher-frequency receiver functions, Tomo - results from tomographic inversion including ambient noise studies.

Author	Refraction	RF	HRF	Tomo	Reflection
Dooley & Moss 1988					X
Collins 1991	X				
Clitheroe et al., 2000		X			
Collins et al. 2003	X				
Reading & Kennett 2003		X			
Reading et al. 2003		X			
Goncharov et al. 2007	X				
Reading et al. 2007		X			
Saygin 2007		X			
Ford et al. 2010		X			
Saygin & Kennett 2010				X	
Kennett et al. 2011		X	X		X
Rawlinson et al. 2011				X	
Reading et al. 2012		X			
Saygin & Kennett 2012				X	
Tkalčić et al. 2012			X		
This work	X	X	X		X

2 DATA SOURCES

The construction of the crustal component of AuSREM has required the assembly of a broad range of information on Australian structure (Table 2), which has then been brought together to generate the actual 3-D model for crustal structure. The various types of data have been used in different ways as discussed below, and have been used with weightings appropriate to the constraints they bring on the 3-D crustal wavespeed distribution (Table 3).

• *Refraction:* We have exploited the full suite of on-shore and off-shore refraction experiments, making use of the data archive at Geoscience Australia, which contains some results that were not included in the studies of Collins et al. (2003) and Goncharov et al. (2007). Finlayson (2010) provides an account of the development of active seismic studies across Australia that has been useful in providing a full range of references up to 2006. Most refraction studies have been carried out with explosive sources, but Bowman & Kennett (1991) were able to exploit the aftershocks of the 1987 Tennant Creek earthquakes on a line to the south and extract a S wavespeed profile.

The information from refraction experiments has a directional component depending on the configuration of the receivers and shotpoints, and we have tried to capture this directionality in the construction of the crustal model even where only a single wavespeed-depth profile is available. In many cases multiple wavespeed profiles have been extracted from a single experiment, and these are all employed. We have used the refraction information as the primary controls on the construction of the crustal model for P wavespeed, but not all of the results have full error estimates for velocities and layer boundaries.

• *Receiver functions:* There have been a number of receiver function studies across the continent, and we have included information from a wide range of sources (see Table 2). In addition we have used some unpublished material, and have extracted a number of additional receiver functions from both portable and permanent stations with the aim of achieving more uniform coverage. In most cases inversion has been carried out directly for a 5-layer crustal model for shear wavespeed and the V_p/V_s ratio using ensemble inversions with either a genetic algorithm (Shibutani et al. 1986) or the Neighbourhood Algorithm (Sambridge 1999).

Receiver function information is specific to the immediate surroundings of the seismic recording stations. The distribution of suitable seismic sources for Australian stations means that there tends to be a bias towards the north and east in the crustal sampling; at the 0.5 degree sampling of the AuSREM model this is not a significant issue. Receiver function inversions provide better constraints on the position of crustal discontinuities than on the absolute velocities, and thus we treat such information as less reliable (see Table 3). Many of the receiver functions have error estimates from the ensemble inversions, but others are based on representations of a single model.

• *Reflection profiles:* More than 12 500 km of full-crust reflection profiles are available across Australia and cover many of the major tectonic provinces (Figure 1). The Moho picks taken at 20 to 40 km intervals along the profiles are very valuable in improving the definition of the Moho depth across Australia (Kennett et al. 2011) and we have incorporated the latest results in the AuSREM model. In addition we have looked for zones of coherent crustal discontinuities in the reflectivity patterns along the reflection profiles.

The control on seismic velocities from the full-crustal reflection work is usually rather poor except in sedimentary areas, and so we have not attempted to use the velocity estimates at depth. We have used the reflection results to provide checks on the sediment distribution and also to relate crustal architecture to the results from other methods.

Table 3. Weighting applied to different classes of data

Data Type	Primary Information	Criterion	Weighting	
Sediment Distribution	h		1.0	
Refraction	V_p		1.0	
Receiver Functions	V_s	Inversion Quality	A: 0.7	B: 0.6
Ambient Noise Tomography	V_s	depth $\leq$ 20 km	0.8	

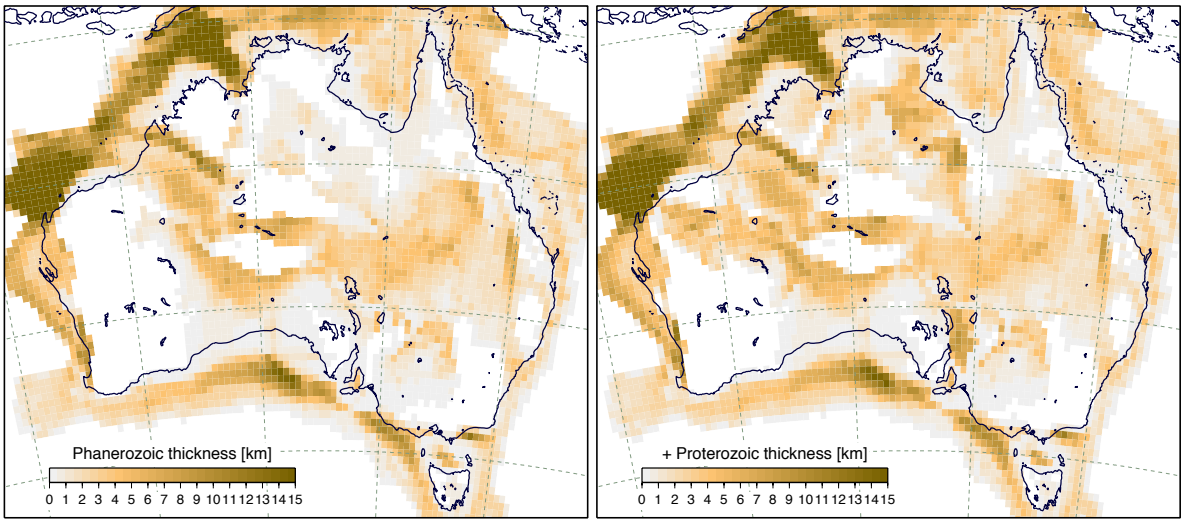

Figure 3. The distribution of Phanerozoic and Proterozoic sedimentary basin thickness across the continent based on the OZSeebase study (Frogtech, 2005) rendered onto the AuSREM 0.5° ×0.5° grid using pixels at the grid size. (a) Phanerozoic and NeoProterozoic basins, (b) with the inclusion of older Proterozoic basins.

- *Tomography:* From the cross-correlation of the ambient noise at pairs of seismic stations we can extract estimates of the Green's functions that would be obtained if one station was a source and the other a receiver. This approach emphasises the surface wave portion of the inter-station response, from which group velocity estimates can be made. With the broad-scale distribution of seismic stations across Australia it is possible to extract path-specific group velocity information that provides good sampling of most of the continent, and then to develop group-velocity maps at a range of periods (Saygin & Kennett 2010). The group velocity dispersion at short-periods is very sensitive to the presence of sediments, and so the group velocity maps provide a useful check on other information on the location of the sediment distribution.

The suite of group dispersion maps for Rayleigh waves can be inverted to provide a 3-D model for crustal S velocities (Saygin & Kennett 2012), using weak constraints on sediment thickness and Moho depth. The resulting shear wavespeed distribution is very valuable as a means of linking the point information across the continent, and so generating a crustal model at the continental scale. This class of information has proved valuable in the construction of the crustal model, and we have given it significant weight down to 20 km (Table 3). Below 25 km depth the estimated S wavespeeds are less reliable, and so we have graded to zero weight at 30 km depth.

Rawlinson et al. (2011) have combined refraction results from a marine survey around the island of Tasmania recorded at land stations with teleseismic data recorded at dense seismic arrays. They have developed a high resolution P-wave tomographic model including a description of the crustal structure and the crust-mantle boundary. The results tie well with the limited results from prior reflection work, and provide a valuable supplement to information on crustal structure in Tasmania.

3 CRUSTAL MODEL

3.1 Sediments

Figure 3(a) displays the thickness of Neoproterozoic and Phanerozoic basins across Australia, building on input from reflection seismology, gravity and magnetic surveys based on Frogtech (2005) with cross-checks against more recent data. We have found that at the 0.5 degree scale of AuSREM, the results from the different sources of information are concordant, but there can be

localised variations of a hundred meters or more. The older Proterozoic sediments are included in Figure 3(b), many of these are metasediments so that the distinction from basement is not always obvious.

Although a significant part of Australia is covered in sediments, the sequences on the continent are generally less than 7 km thick (Figure 3a). Deeper basins (sediment thickness >15 km) occur off-shore particularly in northwestern Australia; they host most of Australia's oil and gas. Nevertheless the onshore basins are important with major coal deposits in eastern Australia, mostly from the Permian, and gas accumulations in the Cooper Basin in southern Queensland. The majority of these basins are associated with gentle downwarps associated with thermal sagging rather than localized rifting, and many in the western part of the continent lie on thick lithosphere. A narrow band of deep sediments occurs in the Fitzroy Trough at the northern end of the Canning basin abutting the Precambrian Kimberly Block. This appears to be an area with periodic tectonic re-activation, and still displays moderate seismicity.

Presently, control on the seismic velocity distributions in the sediments is rather patchy and so we have employed simple models based on compaction. We hope that the availability of AuSREM will encourage the development of more detailed representations of the sedimentary sequences across the continent.

3.2 Construction of model

A major control on the AuSREM crust comes from the P wavespeed (V_p) distribution, largely from refraction experiments. Continental coverages comes from projects from the 1960's to the 1980's, with later efforts off-shore. Additional information has been extracted from receiver function studies via conversion of S wavespeed (V_s) results. As noted above, the absolute velocities from receiver functions have to be treated with caution (see Table 3), but do provide important fill in areas without refraction control. A further important source of information comes from the S wavespeed distribution derived from ambient noise tomography (Saygin & Kennett, 2012) that provides full continental coverage down to about 25 km depth.

The AUSREM crustal model is defined by the P wavespeed (V_p) distribution. The shear wavespeed (V_s) and density (ρ) fields are then constructed from V_p as discussed below. The first contribution to the V_p distribution is constructed from the available refraction results, with the inclusion of receiver function information with lower weight. We restrict the influence of these point data sources to a radius of 250 km about the point and as a result there are some parts of the continent with no control, as well as extensive areas offshore.

3.2.1 Interconversion of V_p and V_s:

The extensive set of receiver function studies using waveform matching provide not only an estimate of S wavespeed (V_s) but also the V_p/V_s ratio. We have developed a representation of the V_p/V_s behaviour by averaging over the receiver functions for groups of stations to develop stable localized estimates for each depth. We then construct a smooth interpolated field across the continent, with the aim of capturing the major variations in V_p/V_s.

In addition to the receiver-function point results, we have also the ambient noise tomography for the S wavespeed distribution (Saygin & Kennett, 2012). The continuous representation across the continent provided by the ambient noise results allows the point observations from receiver functions to be linked, and also the derivation of V_p results in regions of otherwise poor coverage.

We have brought together both the direct V_p results from refraction work, and, on the continent, the values estimated by conversion of V_s using the smoothed estimate of the V_p/V_s ratio. From the combination of these two sets of results, with different geographic coverage, we then construct a smooth estimate of the V_p distribution across the entire model field down to a depth of 25 km. This combined model provides a good representation of the structure. The final S wavespeed model is then constructed by conversion from V_p, and we are then able to check against the original ambient noise and receiver function results and find good consistency.

The procedure is illustrated in Figure 4 in which we show the construction of a detailed V_p field from the ambient noise tomography results, and then its combination with the V_p estimates from refraction and receiver function studies to produce a final V_p distribution with both onshore and offshore coverage. The ambient noise V_p field provides an effective infill for the regions without other coverage. As will be seen from Figures 4 the point measurements and the ambient noise results show good general consistency, with the main differences occurring away from the refraction controls. In consequence the final V_p distribution is not very sensitive to the precise weighting employed between the point and tomographic field results.

Below 25 km depth the reliability of the ambient noise tomographic results diminishes rapidly. For the deeper zone, we therefore use just the estimate of the V_p wavespeeds obtained from refraction results with some lower-weighted supplements from receiver functions.

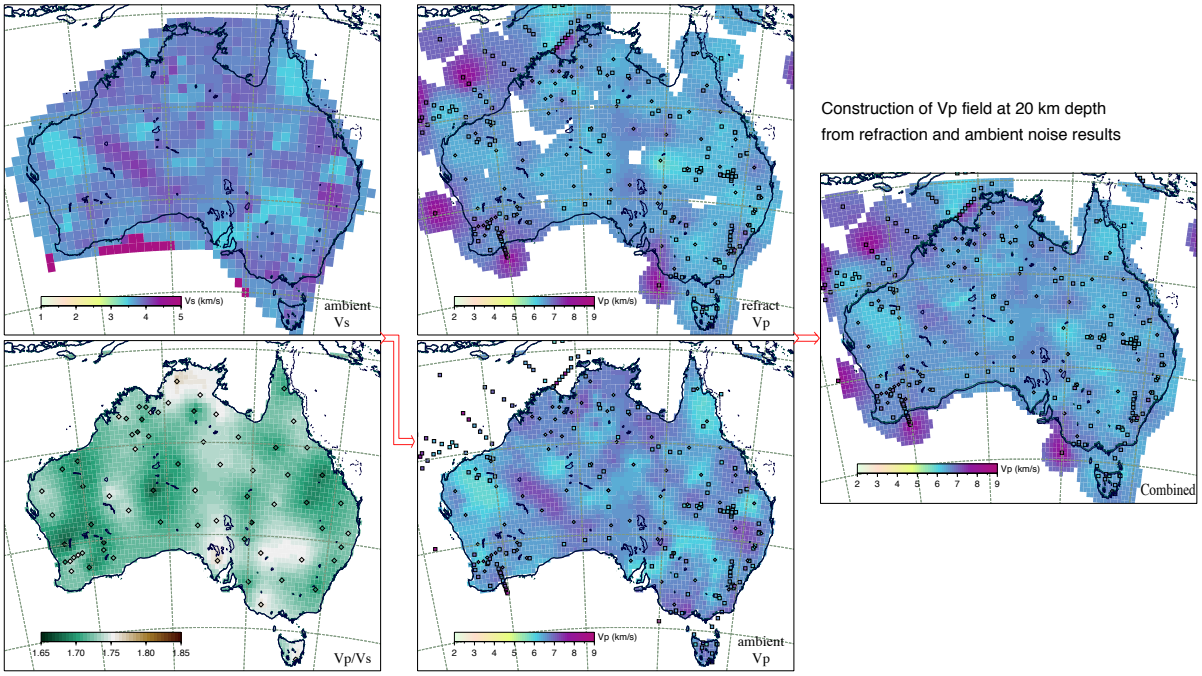

Figure 4. Construction of P model using multiple sources of information, illustrated for the slice at 20 km depth. The ambient noise tomography V_s results of Saygin & Kennett (2102) in conjunction with the smooth V_p/V_s distribution are used to create a V_p distribution for the continet at 05° sampling. This is then combined with the V_p field from refraction and receiver function studies, to produce a V_p field with full coverage.

3.2.2 Relation of Vp and density:

We have followed the conventional approach of linking the density ρ to the P wavespeed V_p. We use an empirical relationship that gives a close fit to the representation proposed by Brocher (2005), but which does not require high powers of V_p:

$$\begin{aligned}
\rho &= 1.150 + 0.400 * V_p - 0.010 * V_p^2, && 1.50 < V_p < 3.00,\\
&= 1.480 + 0.290 * V_p - 0.015 * V_p^2, && 3.00 \le V_p < 4.75,\\
&= 3.258 - 0.395 * V_p + 0.050 * V_p^2, && 4.75 \le V_p < 6.75,\\
&= 4.000 - 0.570 * V_p + 0.060 * V_p^2, && 6.75 \le V_p < 8.50.
\end{aligned}$$

3.2.3 Representation of results:

At each depth we construct a representation of the wavespeed and density distributions, using a combination of the localized results (refraction, receiver functions) and the more distributed tomographic information. The wavespeed or density distributions are constructed using the interpolation tools from the GMT package (Wessel & Smith, 1998) with a conservative approach targeted at 0.5°resolution across the continent. Within each $0.5\times0.5^\circ$ cell we take the weighted results from all relevant estimates; the weighting of the individual data points is based on the data reliability, as specified in Table 3. The weighted means for each cell are then interpolated using an adjustable tension continuous curvature gridding algorithm (Smith & Wessel 1990). The tension factor is set to 0.45 to allow for possible rapid variations. The resulting distribution is displayed allowing the influence of each cellular point to extend no further than 250 km. We blank out areas with no local control.

3.3 Shallow crust

For the shallow crust an important source of information comes from the S wavespeed distribution determined from ambient noise tomography, which has strong sensitivity to the presence of sediments. With the aid of conversion to V_p, this field provides a major supplement to the sparser refraction and receiver function results. Many features of the wavespeed distribution, particularly zones of lower wavespeed are largely controlled by the ambient noise results.

Figure 5 displays the P wavespeed distribution in the AuSREM crust at 5 and 10 km depth, and in Figure 6 we show the equivalent S wavespeed (V_s) distribution We plot the wavespeed estimates from the refraction and receiver function controls on top of the representative wavespeed field, using distinctive symbols for each data type. In both Figures 5 and 6 we see a strong correspondence between the AuSREM crustal model and the point constraints, but in each case a number of significant features can only be mapped because of the availability of the ambient noise tomography. At the shallower depth we see

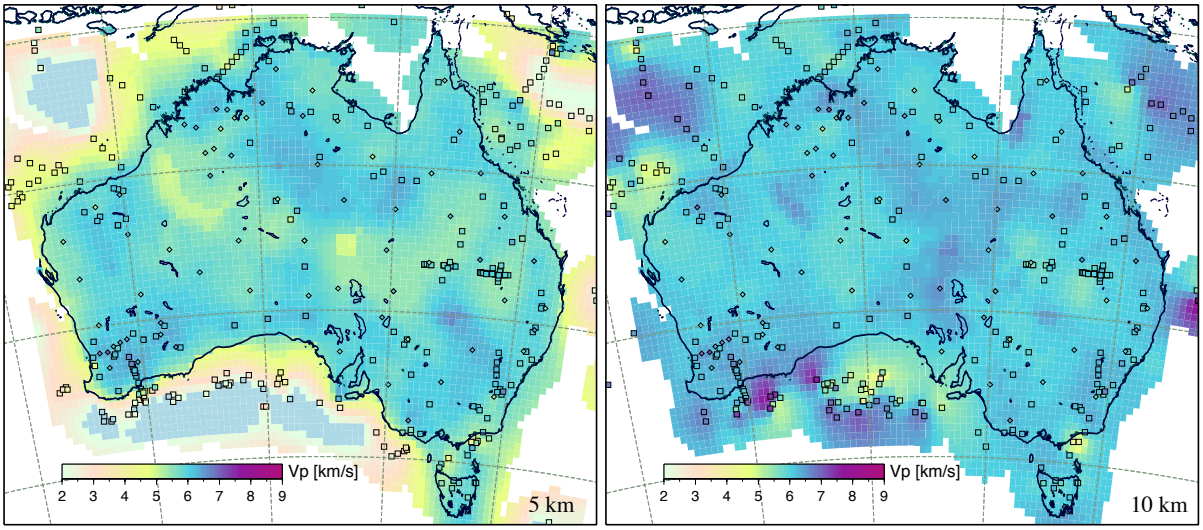

Figure 5. P wavespeed distribution for the AuSREM crustal model at: (a) 5 km depth, (b) 10 km depth. Refraction constraints are indicated by squares and receiver functions information by diamonds, plotted using the same colour scale as the background model. The light blue areas offshore are those with a deep sea bed.

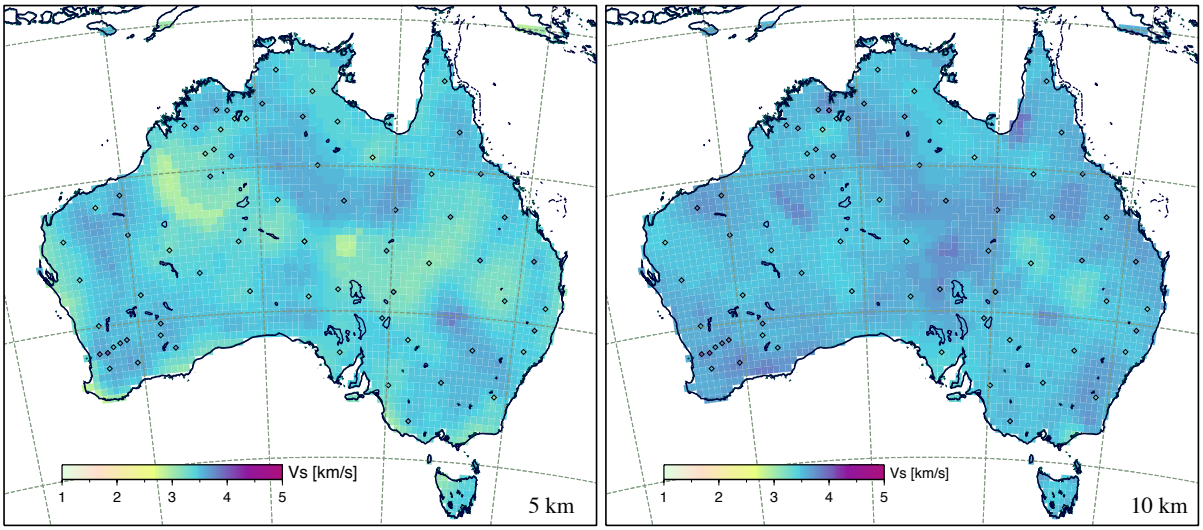

Figure 6. S wavespeed distribution for the AuSREM crustal model at: (a) 5 km depth, (b) 10 km depth. Receiver function constraints are shown by diamonds, plotted using the same colour scale as the background model.

influences from thick sediments, and pick up lower wavespeeds in the Canning Basin and in the Simpson desert. However, limited control means that the thick sediments in the Fitzroy Trough of the Canning Basin are not adequately represented. We simply do not have sufficient information to provide full control on features whose smallest dimension is of the order of 100 km, unless specific experiments are in the locality.

At 10 km depth offshore in some parts we have reached lower crustal velocities. On the whole seismic wavespeeds across the continent are quite high even at 5 km depth, with P wavespeed approaching 6 km/s. The wavespeeds continue to increase, but more slowly, to 10 km depth.

Figure 6 shows the S wavespeed distribution derived from the V_p model, and in Figure 7 we illustrate the associated V_p/V_s ratios distribution across the Australian continent. As might be expected, the V_s wavespeed at 5 and 10 km depth largely mirrors V_p. There are, however, distinct differences such as the relatively higher S wavespeeds in the Pilbara and along the eastern seaboard,

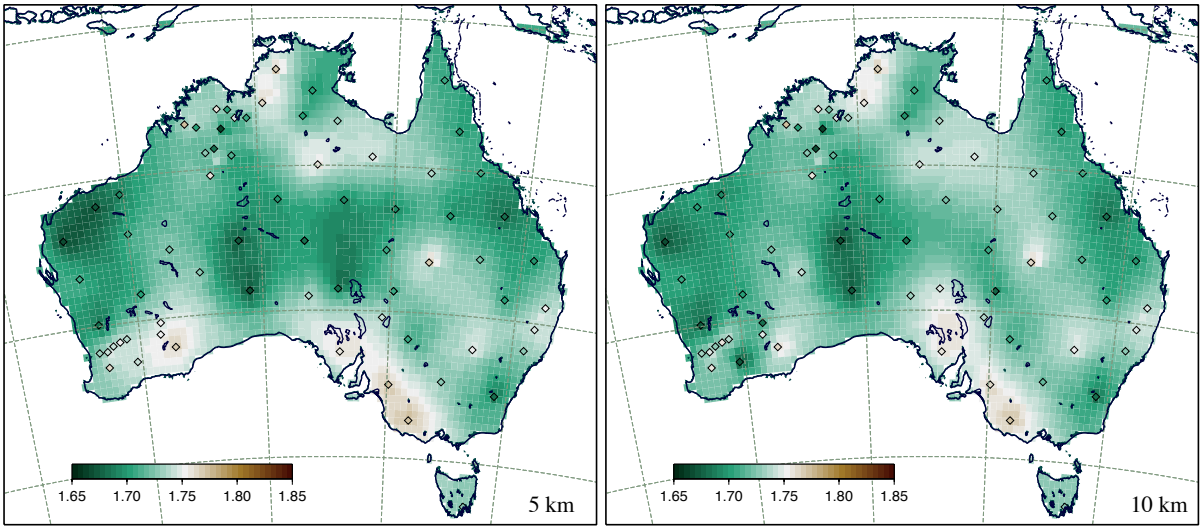

Figure 7. V_p/V_s ratio distribution for the AuSREM crustal model at: (a) 5 km depth, (b) 10 km depth. The location of the receiver function constraints are indicated by diamonds, plotted using the same colour scale as the background ratio model.

3.4 Deeper crust

The ambient noise tomography provides continent wide coverage down to 25 km depth, but becomes less reliable at greater depth because of limited controls for longer period noise (Saygin & Kennett, 2012). Below 25 km we depend on refraction and receiver function information with a more limited spatial distribution. In Figure 8 we blank out areas that lie beyond 250 km from any control point, but the AuSREM crustal model is continuous and wavespeed can be extracted at any point.

In Figure 8 we display the V_p distribution in the deeper crust with slices at 15, 20, 25 and 30 km depth. This is accompanied by the V_s distribution at 15 and 25 km in Figure 9, and the V_p/V_s ratio field at the same depths in Figure 10. The S wavespeed distribution is generally similar to that for V_p, because the variations in the V_p/V_s ratio are not very large even though they show distinct geographic patterns. There are some localised variations in the patterns of V_p and V_s gradients arising from the spatial variations of V_p/V_s.

By 30 km depth, we see a generally good correlation of the pattern of P wavespeed with the depth to Moho (Figure 15). Areas with thicker crust commonly have lower V_p than where the crust is thinner. Nevertheless, relatively high wavespeed are seen in the Lachlan Fold Belt where it is likely that a thickened lower crust has been assembled by underplating. It is interesting to note a distinct edge emerge along the southern margin of the Kimberly region with a contrast between high and lower wavespeeds. This zone lies below the Fitzroy Trough with a narrow zone of rather thick sediments (Figure 3).

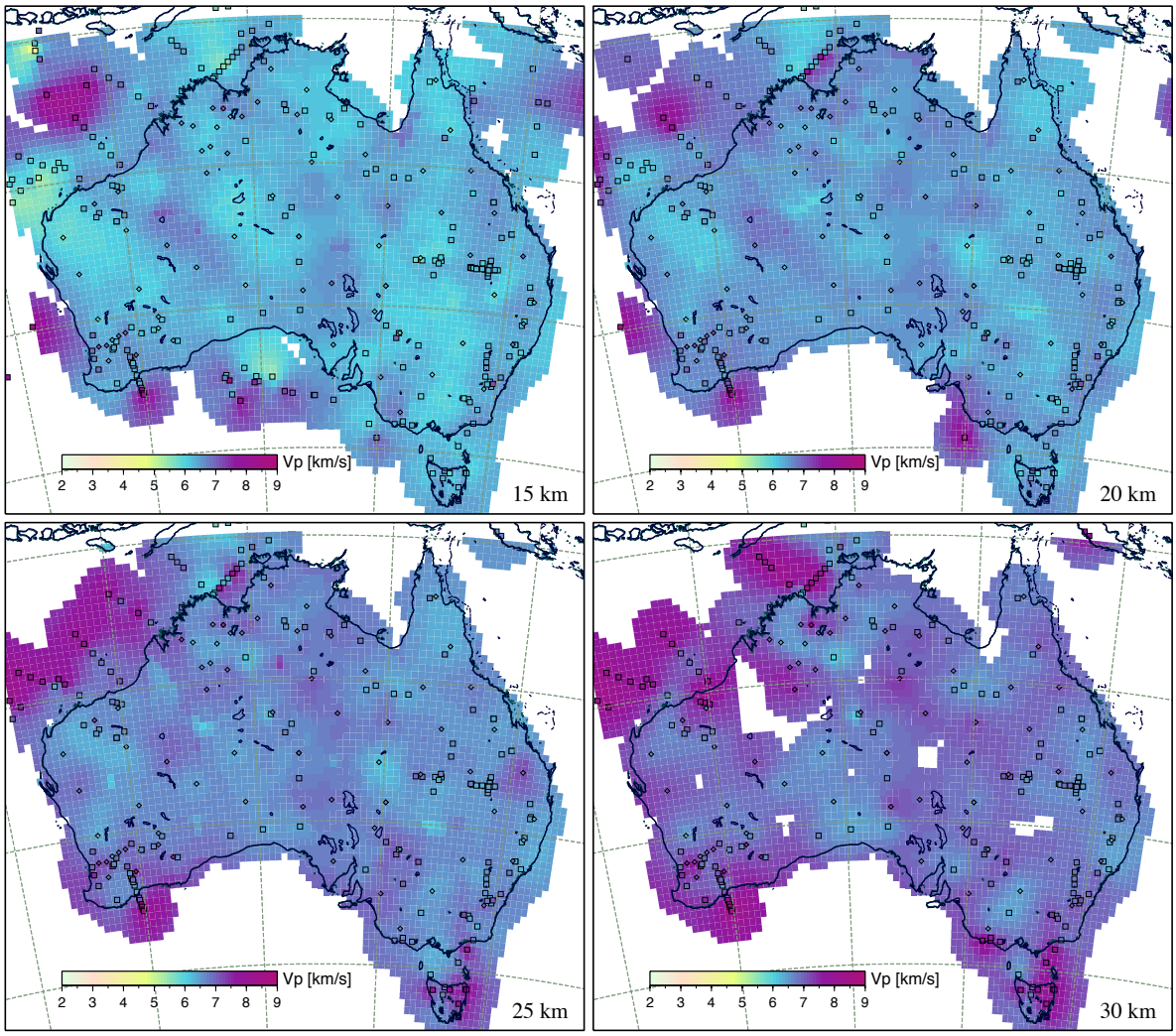

Figure 8. P wavespeed distribution for the AuSREM crustal model at: (a) 15 km depth, (b) 20 km depth, (c) 25 km depth, (d) 30 km depth. Refraction constraints are indicated by squares and receiver functions information by diamonds, plotted using the same colour scale as the background model. We blank out the portions of the deeper slice where there are no local constraints, the model itself is continuous but less reliable in such regions.

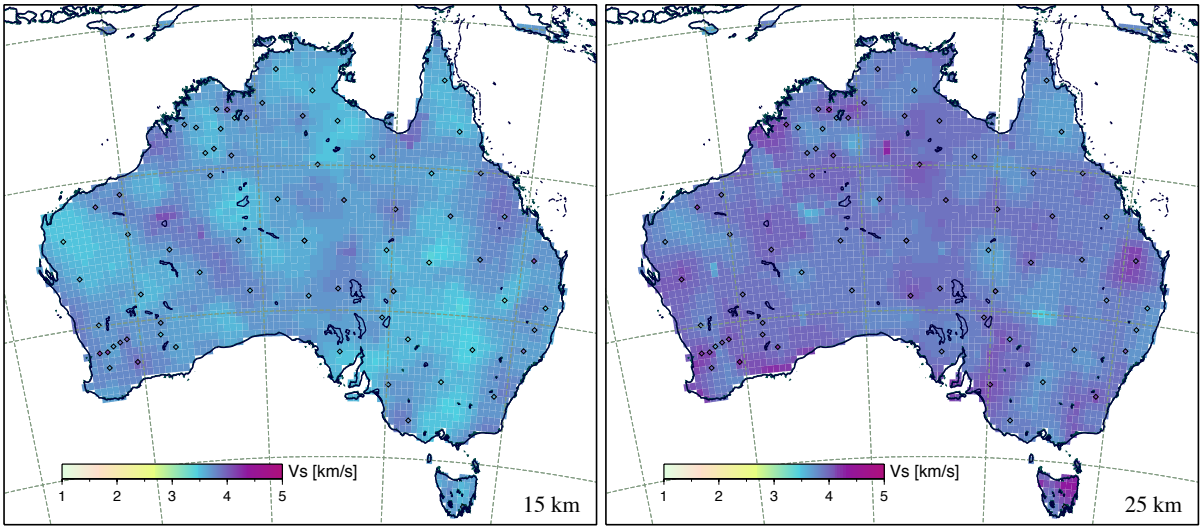

Figure 9. S wavespeed distribution for the AuSREM crustal model at: (a) 15 km depth, (b) 25 km depth. Receiver function constraints are shown by diamonds, plotted using the same colour scale as the background model.

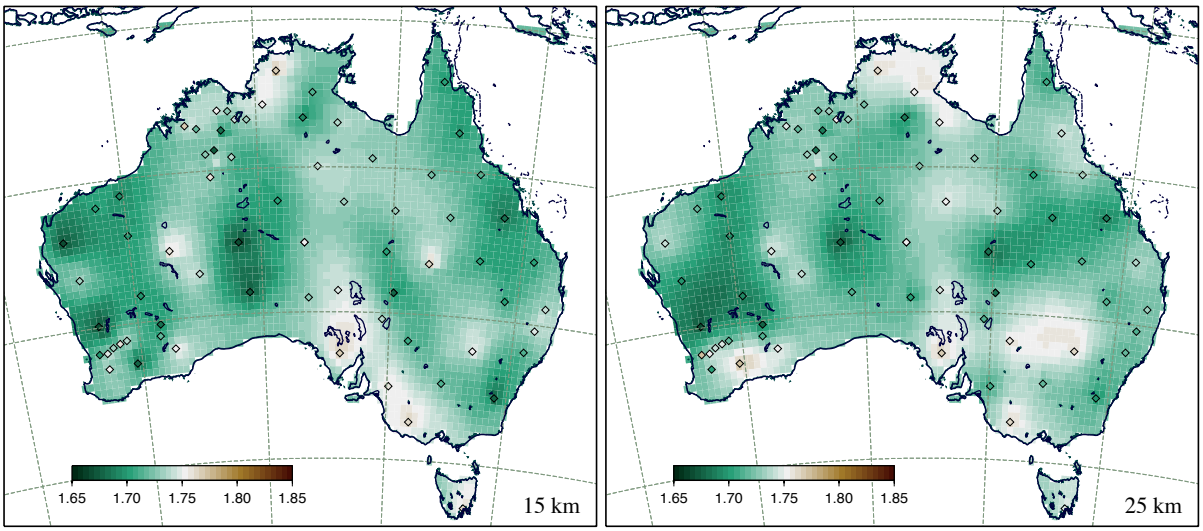

Figure 10. V_p/V_s ratio distribution for the AuSREM crustal model at: (a) 15 km depth, (b) 25 km depth. The location of the receiver function constraints are indicated by diamonds, plotted using the same colour scale as the background ratio model.

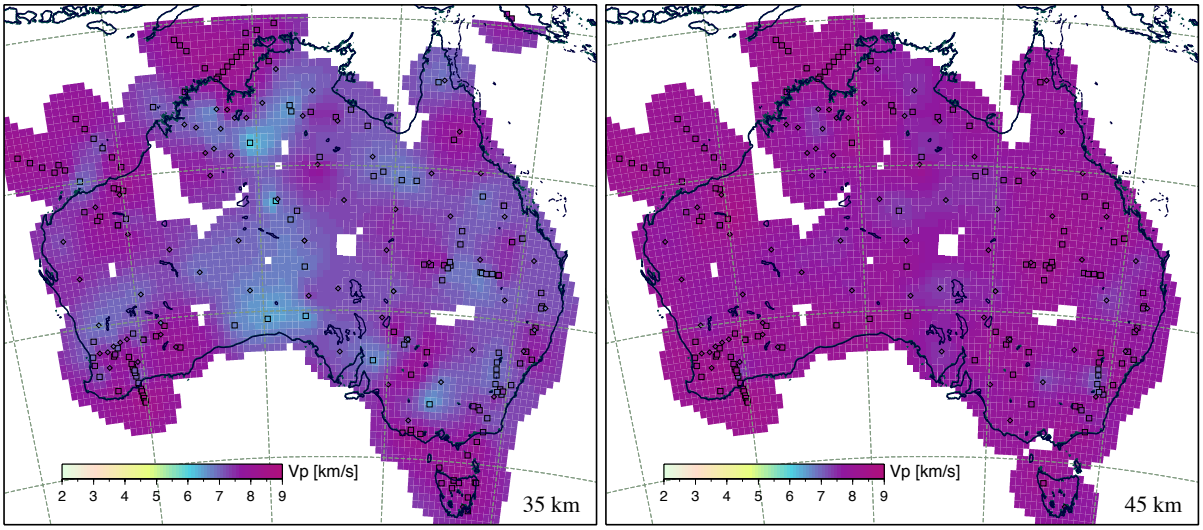

Figure 11. P wavespeed distribution for the AuSREM crustal model at: (a) 35 km depth, (b) 45 km depth. Refraction constraints are indicated by squares and receiver functions information by diamonds, plotted using the same colour scale as the background model.

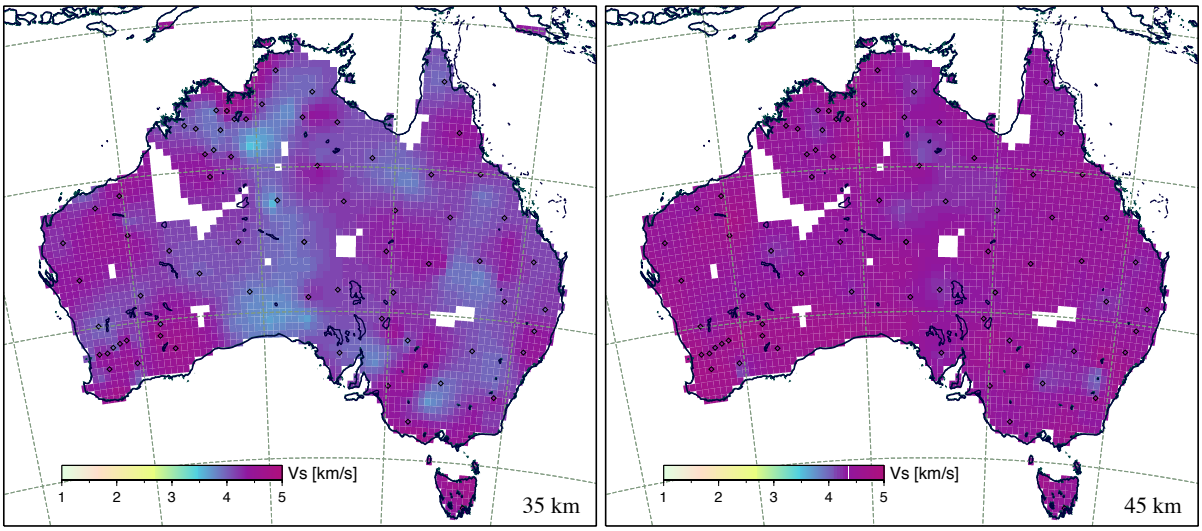

Figure 12. S wavespeed distribution for the AuSREM crustal model at: (a) 35 km depth, (b) 45 km depth. Receiver function constraints are shown by diamonds, plotted using the same colour scale as the background model.

3.5 Base of crust and uppermost mantle

The thinnest parts of the crust in the Pilbara and the Lake Eyre basin are around 30 km thick (see Figure 15). Thus at any greater depth we are cutting through both crustal and uppermost mantle materials. We illustrate this portion of the AuSREM model in Figures 11–13, where we display depth slices at 35 and 45 km for the P wavespeed, S wavespeed and V_p/V_s ratio.

There is a significant shift to higher seismic wavespeed between 35 and 45 km depth. The influence of the areas of thicker crust are evident at 35 km, but we must recall that our velocity controls are rather patchy. Thus the deeper wavespeed distribution in many parts of the continent is only poorly constrained. The longest wavelength components are likely to be reasonably well represented, but local gradients will be significant only where we have data points. Most of the squares for refraction results and the diamonds for receiver functions are essentially invisible in Figure 11, 12, because they blend so well with the background model.

The V_p/V_s ratio distribution shown in Figure 13 shows a marked shift to higher values compared with shallower depths. Ratios around 1.8 are characteristic of the uppermost mantle, but can be encountered toward the base of the crust in regions with a gradational transition from crust to mantle, as in the Northern Australian craton at around 20°S.

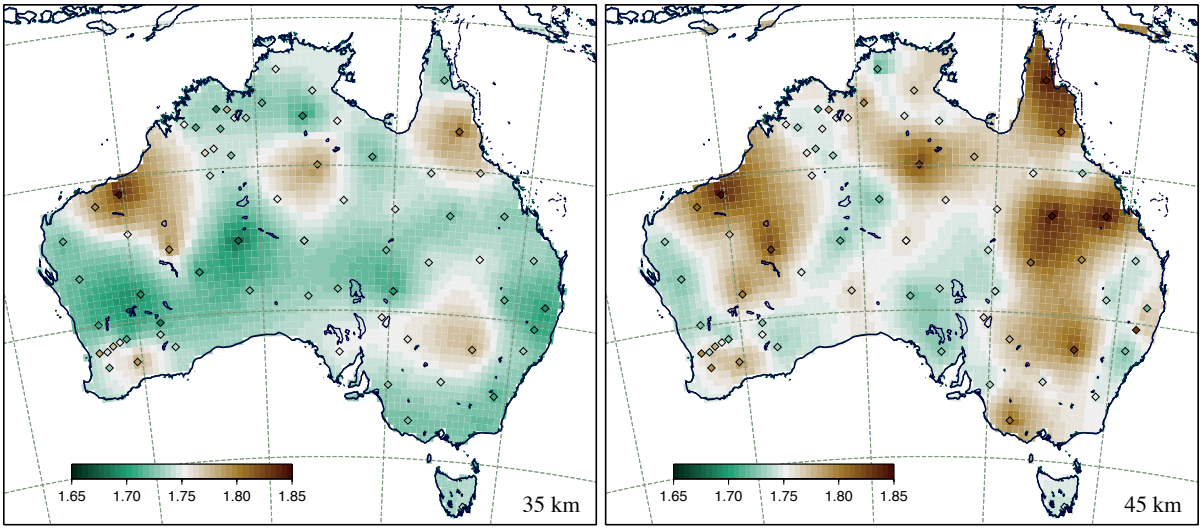

Figure 13. V_p/V_s ratio distribution for the AuSREM crustal model at: (a) 35 km depth, (b) 45 km depth. The location of the receiver function constraints are indicated by diamonds, plotted using the same colour scale as the background ratio model.

3.6 Crustal discontinuities

The representation of crustal structure presented in Table 1 allows for the possibility of discontinuities separating the gradient zones. However, we have not not found evidence for any coherent discontinuity across the continent, so there is no simple divide between the upper and lower parts of the crust. We have carried out a thorough search through the record sections for all of the full crustal reflection profiles, and the interpreted wavespeed profiles from both refraction and receiver function studies. Many discontinuities can be recognised as can be seen in Figure 14, but few features have more than a limited extent. We show the discontinuity estimates in bands of 9 km thickness; such a division is rather arbitrary but helps to reveal the full pattern since there may be two discontinuities present at a single locality. Discontinuities occur at all levels in the crust and we do see some regional clustering such as the discontinuity at around 24 km depth in southern Queensland seen in both reflection and refraction studies (Finlayson et al., 1984). There is also a cluster of deep crustal discontinuities in the southern Yilgarn craton in the west (cf. Dentith et al., 2000).

On reflection profiles we often see relatively clear reflectors marking the top and bottom of a zone of distinctive crustal reflectivity rather than a simple mid-crustal division. It is rare for a coherent reflector to persist for more than 200 km before the style of reflectivity changes. Even when clear, the prominent reflectors can show significant topography as in the Youanmi province of the northern Yilgarn craton, where they vary by more than 6 km in depth along a single recognisable interface, marking a distinct change in reflection character.

In most cases the refraction and receiver function results are rather sparse so that it is difficult to judge the level of horizontal continuity, but as can be seen in Figure 14 some regional trends are apparent.

3.7 Moho

Kennett et al. (2011) provide a detailed description of the construction of the model of Moho depth drawing on the full range of seismological information (Figure 1), including refraction, receiver function and reflection studies. This model has been updated to include results from reflection experiments in Western Australia in 2012, across the Albany-Fraser belt, which provide detailed information in an area where previously there was little constraint. These new results have required a reconsideration of prior estimates of crustal thickness. It would appear that at some sites a deep crustal discontinuity has been identified as the Moho, and these picks are now included in Figure 14 as crustal discontinuities. The basal crustal layer in this area has a rather high velocity, so that it is on the margin of the criterion used for declaring a Moho pick.

The updated Moho model is displayed in Figure 15 in the same configuration as for the other crustal elements. As can be clearly seen there is a significant area of thick crust (Moho depth greater than 40 km) in central Australia, with the depth to Moho exceeding 50 km in places. In a number of places there are sharp jumps in Moho depth of 10 km or more (see, e.g., Goleby et al. 1989). Such features cannot be adequately represented by a smooth Moho surface, even though as can be seen in Figure 15 there are distinct regions with strong horizontal gradients in Moho depth. With the new results from the Albany-Fraser belt, we now see a clear wrap of slightly thickened crust around the southern margin of the Yilgarn craton, a feature that may well be derived from the original orogeny at around 1400 Ma.

The Moho model provides a direct link between the crustal and mantle components of AuSREM. The pattern of wavespeed

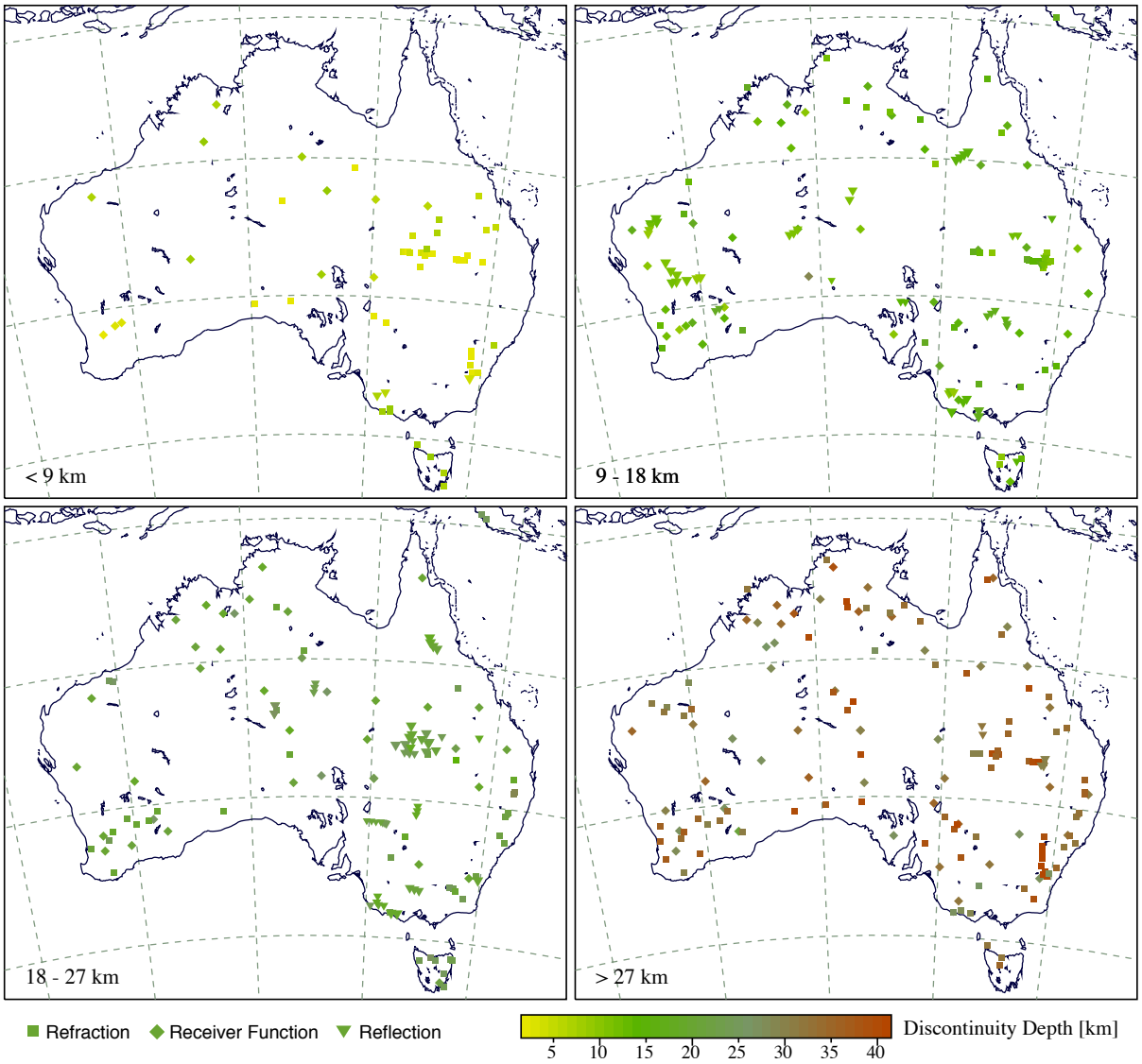

Figure 14. Estimates of depth to crustal discontinuities extracted from the full set of available seismological information including reflection profiles, refraction and receiver function studies. Different shapes of symbols are used for the different classes of data as indicated in the key below. The panels represent 9 km intervals so that multiple discontinuities at the same location can be seen.

at 50 km depth is largely controlled by Pn results from refraction experiments, which are themselves sparse. Unfortunately the constraints on the nature of the uppermost mantle are relatively weak, particularly since the influence of crustal structure in surface wave tomography is rather strong at such depths.

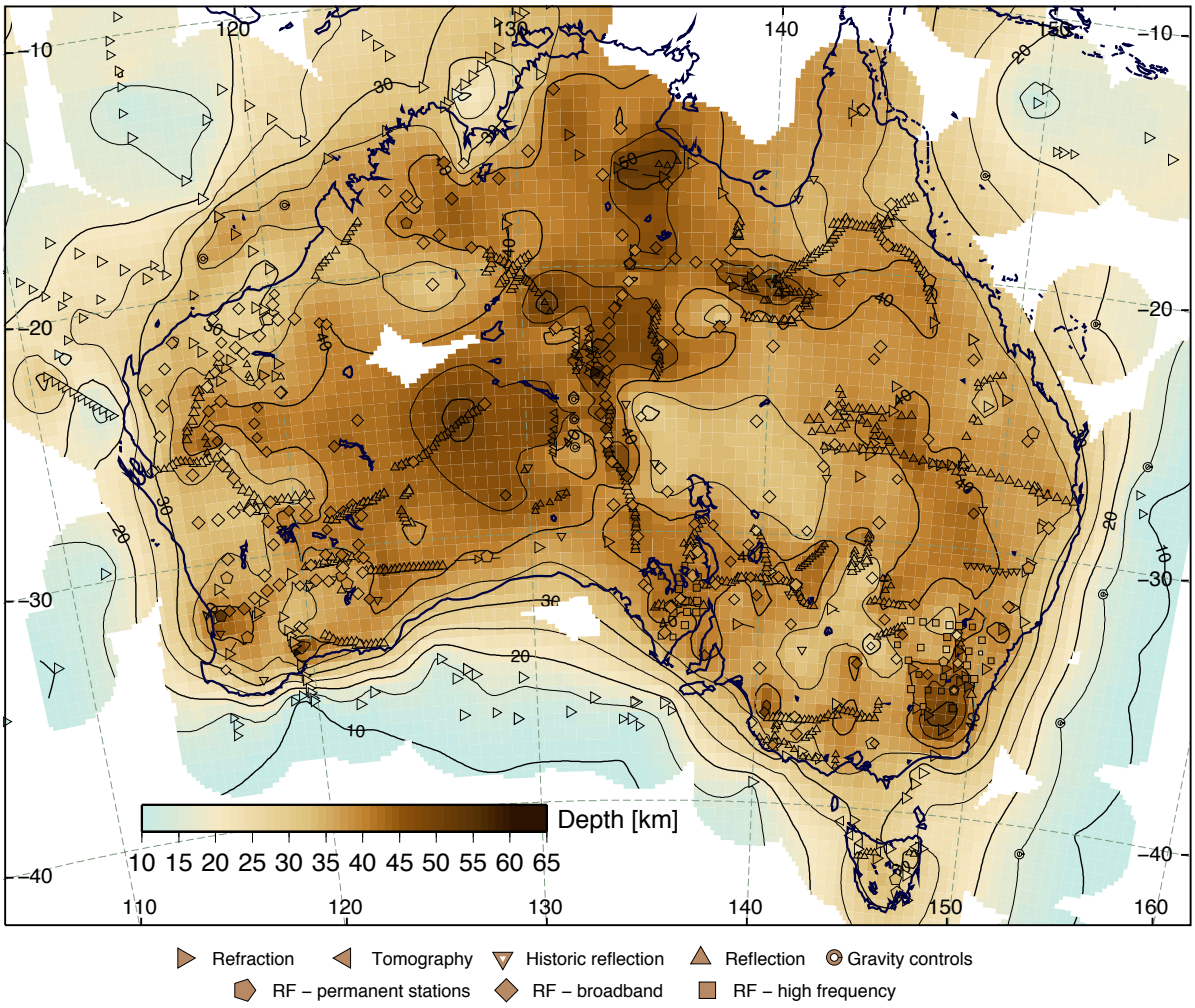

Figure 15. Moho surface constructed from the full set of available seismological estimates to mid 2012 (updated from Kennett et al., 2011). The surface is constructed by interpolating weighted averages for each 0.5°×0.5° cell, the size of the pixels in the image. The original results are superimposed on the interpolated surface using the same colour coding, shown at the right with depths in kilometres. Different shapes of symbols are used for the various classes of data as indicated in the key below, the size indicates the relative weighting applied to the data point. Additional control points based on the gravity analysis by Aitken (2010) are indicated by double circles; these extra points, applied with low weighting, help define features with strong east-west directionality in central Australia, and constrain, to some extent, the continent-ocean margin to the east of Australia.

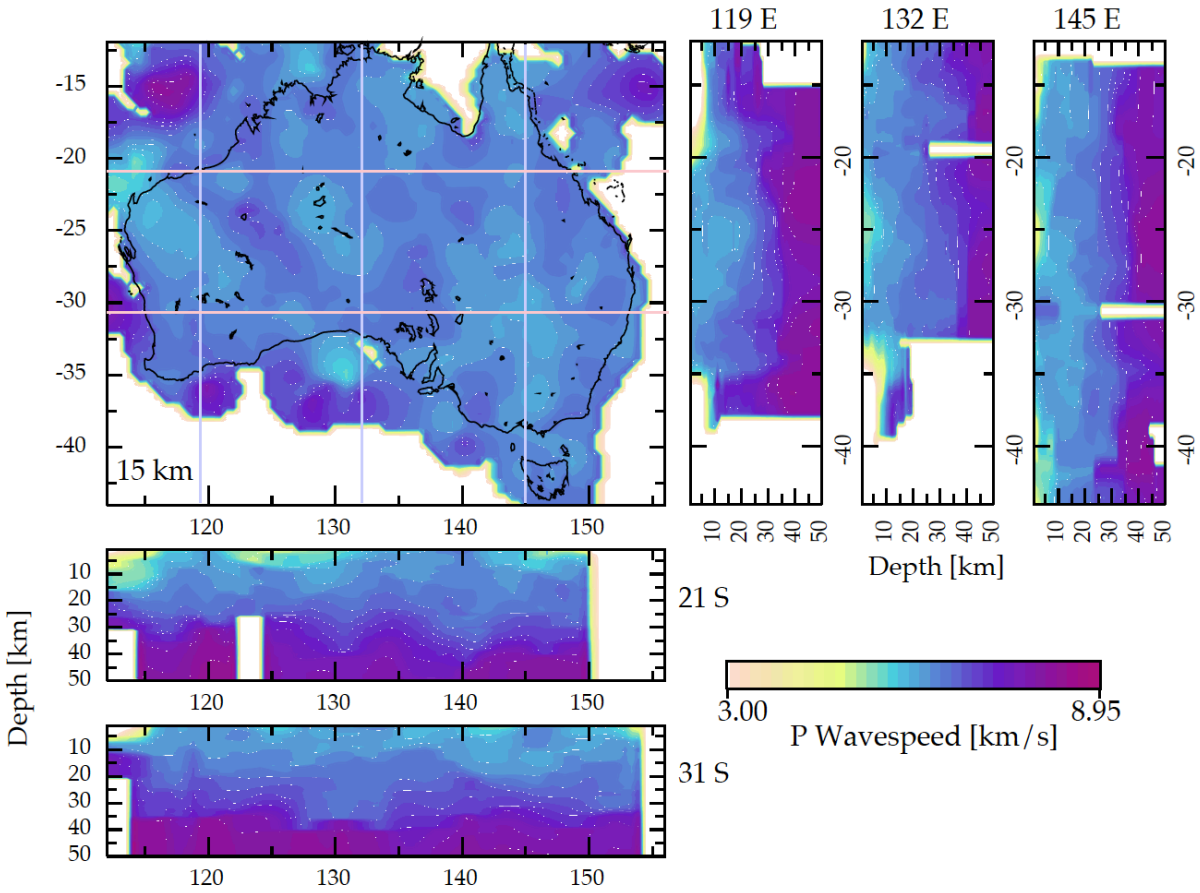

Figure 16. Cross-sections through the AUSREM crustal model, along the lines indicated on the key map showing a map view at 15 km depth. Sections are shown at 21°S, 31°S and at 119°E, 132°E, 145°E.

4 DISCUSSION

The different tectonic elements of Australia are most evident in shallow wavespeed structure and there is less correspondence below 10 km depth. Instead one can begin to recognise distinctive domains within the tectonic features, characterised by variations in wavespeed. Such a partitioning of crustal structure has been identified by Reading et al. (2003) from receiver function studies. The new crustal model indicates that this concept has wider validity, so that, e.g., in the mid-crust a number of broad areas of similar character can be recognised in the North Australian craton.

In Figure 16 we show a set of cross-sections through the AUSREM crustal model, keyed to a map view at 15 km depth. The sections at 21°S, 31°S and 119°E, 132°E, 145°E have been chosen to provide profiles across as much of the continent as possible whilst sampling a variety of tectonic provinces. As in the earlier map views we blank out regions without adequate constraint; which is why we have the apparent notches below 25 km depth in the cross-sections. The same parallels and meridians have also been employed for the mantle component of AuSREM in Kennett et al. (2012), but here the domain extends further away from the continent.

In the 21°S section from west to east the profile crosses the Northwest Shelf and the Pilbara. Then the Canning basin is evident by the lower P wavespeed in the sediments, followed by a large slice of the North Australian craton, with just a narrow strip of Phanerozoic on the east coast. The thickened crust in the northern part of Central Australia and the Mt. Isa block are evident through the projection of lower wavespeeds to greater depth. The 31°S section starts in the Yilgarn craton, crosses the little known zone of the Eucla basin, the Galwer Craton and on the eastern seaboard the Lachlan Fold Belt. Between 123°E and 142°E, the profile lies mostly within thicker crust. The complex gradient in the Moho structure near 134°E is reflected in distinct horizontal gradients in P wavespeed.

The north-south sections sample the West Australian cratons and the Capricorn orogen at 119°E, the full extent of the North and South Australian cratons at 132°E, and the Phanerozoic tectonic belts at 145°E. Thick sedimentary sequences appear near 25°S in both the central and eastern sections. There is much to digest in the rich patterns of the wavespeed distributions, and we hope that their availability with stimulate further study of the full crustal section.

5 CONCLUSIONS

The AuSREM project provides a description of the major features of the Australian lithosphere. The structure is designed to be representative, and has been based on the combination of many different lines of evidence. The aim has been to provide a good representation of 3-D structure, which is useful for applications yet is presented in a way that can be refined as extra information becomes available.

With the aid of the results from ambient noise tomography (Saygin & Kennett, 2012), we can achieve full continental coverage to 25 km. At greater depth and offshore, we have to rely on sparse information dominantly from refraction experiments. Some of the broad tectonic features of the continent can be recognised in the wavespeed distributions in the upper part of the crust, but are less evident at depth.

Discontinuities within the crust tend to be localised and occur at many different depths. The Moho, the major boundary in the upper lithosphere, is highly variable in its character and depth below the surface. Depths to Moho across the continent range from 25–60 km, despite an average elevation of only ~330 m above sea level. There are rapid variations in crustal thickness in central Australia that give rise to major east-west oriented gravity anomalies. The character of the transition from crust to mantle is highly variable with extended gradients accompanying the deepest Moho, probably associated with mafic underplating. There is no simple relationship between depth to Moho and crustal age, though many of the zones of thickest crust are in regions of Proterozoic outcrop.

The AuSREM model provides a continuous representation of the crustal structure for the Australian continent and its immediate surroundings, represented on a 0.5° horizontal grid and closely spaced in depth. In consequence crustal properties can be extracted at any position. Nevertheless, we have to recognise the limitations in the model. We do not have dense P wavespeed information in the crust across the continent, and have had to enhance the limited number of refraction results with P wavespeed derived from the conversion of S wavespeeds from receiver functions and ambient noise tomography. We have then constructed the AuSREM S wavespeed and density components from the final P wavespeed distribution. As we have seen, the model is internally consistent, but undoubtedly will prove to be limited in many areas as new data becomes available.

In addition to the specific results we have been able to assemble for the wavespeed distribution in the crust, the new crustal component of AuSREM will be useful in a number of other ways, e.g., in gravity modelling and studies of dynamic topography. The influence of crustal structure is significant for much of the frequency band used in surface wave tomography to study the lithospheric mantle and the asthenosphere beneath, and better crustal corrections will aid future studies. The crustal model will also provide a useful starting point for delay time tomography on a finer scale.

6 THE AUSREM MODEL

The AuSREM model is presented in full at the web-site
http://rses.anu.edu.au/seismology/AuSREM
from which the model can be downloaded in a number of formats, and where it is also possible to generate maps and depth profiles. The web site also includes information on the refraction experiments and receiver function profiles employed in this study.

ACKNOWLEDGEMENTS

The AuSREM project has been jointly supported by AuScope and the Research School of Earth Sciences, Australian National University. We would like to thank Clive Collins and Alexei Gorbatov at Geoscience Australia for access to their database of refraction results and to their unpublished estimates of the crustal velocity distribution. Fabrice R. Fontaine and Liz Vanacore have kindly provided their unpublished receiver function studies.

Funding support for the passive seismic work has been provided from the Australian National University, from Discovery Projects funded by the Australian Research Council, from the Predictive Mineral Discovery Cooperative Research Centre, and the AuScope infrastructure initiative. The active seismic work was initiated by the Bureau of Mineral Resources (subsequently Australian Geological Survey Organisation and now Geoscience Australia). The recent surveys have been funded through the Australian Government Onshore Energy Security Program, the AuScope infrastructure initiative and State investments from Queensland, Western Australia, South Australia, New South Wales and Victoria.

REFERENCES

Aitken, A.R.A., 2010. Moho geometry gravity inversion experiment (MoGGIE): A refined model of the Australian Moho and its tectonic and isostatic implications, *Earth Planet. Sci. Lett.*, **297**, 71–83.

Betts, P.G., Giles, D., Lister, G.S. & Frick, L.R., 2002. Evolution of the Australian Lithosphere, *Austral. J. Earth Sci.*, **49**, 661–692.

Bowman, J.R. & Kennett, B.L.N., 1991. Propagation of *Lg* waves in the North Australian craton: influence of crustal velocity gradients, *Bull. Seism. Soc. Am.*, **81**, 592–610.

Brocher, T.M., 2005. Empirical relations between elastic wavespeeds and density in the Earth's crust, *Bull. Seism. Soc. Am.*, **95**, 2081–2092.

Cawood, P. & Korsch, R.J., 2008. Assembling Australia: Proterozoic building of a continent, *Precambrian Res.*, **166**, 1–38.

Clitheroe, G., Gudmundsson, O. & Kennett, B.L.N., 2000. The crustal thickness of Australia, *J. Geophys. Res.*, **105**, 13 697–13 713.

Collins, C.D.N., 1991. The nature of the crust-mantle boundary under Australia from seismic evidence, *The Australian Lithosphere*, edited by B.J. Drummond, Spec. Publ., Geol. Soc. Aust., **17**, 67–80.

Collins, C.D.N., Drummond, B.J., & Nicoll, M.G., 2003. Crustal thickness patterns in the Australian continent, 121–128, in *The Evolution and Dynamics of the Australian Plate*, Ed. D. Müller & R. Hillis. Geological Society of Australia Special Publication **22** and Geological Society of America Special Paper **372**.

Collins, W.J. & Vernon, R.H., 1992. Palaeozoic arc growth, deformation and migration across the Lachlan Fold Belt, southeastern Australia. *Tectonophys.*, **214**, 381–400.

Dentith, M.C., Dent V.F. & Drummond B.J. 2000. Deep crustal structure in the southwestern Yilgarn Craton, Western Australia. *Tectonophys.*, **325**, 227?-255.

Direen, N.G. & Crawford, A J., 2003. The Tasman Line: where is it, what is it, and is it Australia's Rodinian breakup boundary?, *Austral. J. Earth Sci.*, **50**, 491–502.

Dooley, J.C. & Moss, F.J. 1988. Deep crustal reflections in Australia 1957-1973 - II. Crustal models , *Geophys. J. R. Astr. Soc.*, **293**, 239–249.

Finlayson, D.M., 2010. *A Chronicle of Deep Seismic Profiling across the Australian Continent and its Margins, 1946-2006*, D.M. Finlayson, Canberra, pp 255 (doug.finlayson@netspeed.com.au).

Finlayson, D.M., Collins, C.D.N. & Lock, J., 1984. P-wave velocity features of the lithosphere under the Eromanga Basin, eastern Australia, including a prominent mid-crustal (Conrad?) discontinuity. *Tectonophys.*, **101**, 267–291.

Fishwick, S., Heintz, M., Kennett, B.L.N., Reading, A.M. & Yoshizawa, K., 2008. Steps in lithospheric thickness within eastern Australia, evidence from surface wave tomography, *Tectonics*, **27**, TC0049, doi:10.129/2007TC002116.

Ford, H.A., Fischer, K.M., Abt, D.L., Rychert, C.A. & Elkins-Tanton, L.T., 2010. The lithosphere-asthenosphere boundary and cratonic lithospheric layering beneath Australia from *Sp* wave imaging, *Earth Planet. Sci. Lett.*, **300**, 299–310.

Frogtech, 2005. OZ SEEBASE™ Study 2005, Public Domain Report to Shell Development Australia by FrOG Tech Pty Ltd.

Goleby, B.R., Shaw, R.S., Wright, C., Kennett, B.L.N. & Lambeck, K., 1989. Geophysical evidence for 'thick-skinned' crustal deformation in central Australia, *Nature*, **337**, 325-330.

Grad, M., Tiira, T. & ESC Working Group, 2009. The Moho depth map of the European Plate, *Geophys. J. Int.*, **176**, 279-292.

Goncharov, A., Deighton, I., Tischer, M. & Collins, C., 2007. Crustal thickness in Australia: where, how and what for?, *ASEG Extended Abstracts, Perth, Western Australia*.

Kennett, B.L.N. 2003, Seismic Structure in the mantle beneath Australia, 7–23, in *The Evolution and Dynamics of the Australian Plate*, Ed. D. Müller & R. Hillis. Geological Society of Australia Special Publication **22** and Geological Society of America Special Paper **372**.

Kennett, B.L.N., Fishwick, S., Reading, A.M. & Rawlinson, N., 2004. Contrasts in mantle structure beneath Australia relation to Tasman Lines?, *Austral. J. Earth Sci.*, **51**, 563–569.

Kennett, B.L.N., Salmon, M., Saygin, E. & AusMoho Working Group, 2011. AusMoho: the variation of Moho depth in Australia, *Geophys. J. Int.*, **187**, 946–958.

Kennett, B.L.N. & Salmon, M., 2012. AuSREM: Australian Seismological Reference Model, *Austral. J. Earth. Sci.*

Kennett, B.L.N., Fichtner, A., Fishwick, S. & Yoshizawa, K. 2012, The Australian Seismological Reference Model (AUSREM): Mantle component. *Geophys. J. Int.*,

Moss, F.J. & Dooley, J.C. 1988. Deep crustal reflection recordings in Australia 1957-1973 - I. Data acquisition and presentation, *Geophys. J. R. Astr. Soc.*, **293**, 229–238.

Rawlinson, N., Tkalčić, H. & Reading, A.M., 2011. Structure of the Tasmanian lithosphere from 3D seismic tomography, *Austral. J. Earth Sci.*, **57**, 381–394.

Rawlinson, N., Kennett, B.L.N., Vanacore, E., Glen, R.A., & Fishwick, S., 2011. The structure of the upper mantle beneath the Delamerian and Lachlan orogens from simultaneous inversion of multiple teleseismic datasets, *Gondwana Res.*, **19**, 788–799.

Reading, A.M., Kennett, B.L.N. & Dentith, M.C. 2003. The seismic structure of the Yilgarn Craton, Western Australia, *Austral. J. Earth Sci.*, **50**, 427–438.

Reading, A.M. & Kennett, B.L.N., 2003. Lithospheric structure of the Pilbara Craton, Capricorn Orogen and northern Yilgarn Craton, Western Australia, from teleseismic receiver functions, *Austral. J. Earth Sci.*, **50**, 439–445.

Reading, A.M., Kennett, B.L.N. & Goleby, B., 2007. New constraints on the seismic structure of West Australia: Evidence for terrane stabilization prior to the assembly of an ancient continent?, *Geology*, **35**, 379–379.

Reading, A.M., Tkalčić, H., Kennett, B.L.N., Johnson, S.P. & Sheppard, S. 2012. Seismic structure of the crust and uppermost mantle of the Capricorn and Paterson Orogens and adjacent cratons, Western Australia, from passive seismic experiments, *Precambrian Research*, **196**, 295–308.

Sambridge, M.S., 1999. Geophysical inversion with a neighbourhood algorithm – I. Searching a parameter space, *Geophys. J. Int.*, **138**, 479–494.

Sandiford M. 2003, Neotectnics of southeastern Australia: linking the Quaternary faulting record with seismicity and *in-situ* stress, 107–119, in *The Evolution and Dynamics of the Australian Plate*, Ed. D. Müller & R. Hillis. Geological Society of Australia Special Publication **22** and Geological Society of America Special Paper **372**.

Saygin, E., 2007. *Seismic Receiver and Noise Correlation Based Studies in Australia*, Ph.D. Thesis, The Australian National University.

Saygin E. & Kennett B.L.N., 2010. Ambient noise tomography for the Australian Continent. *Tectonophys.*, **481**, 116–125.

Saygin, E. & Kennett, B.L.N., 2012. Crustal structure of Australia from ambient seismic noise tomography. *J. Geophys. Res.*, **117**, B01304, doi:10.1029/2011JB008403.

Shibutani, T., Sambridge, M., & Kennett, B., 1996. Genetic algorithm inversion for receiver functions with application to crust and uppermost mantle structure beneath eastern Australia, *Geophys. Res. Lett.*, **23**, 1829–1829.

Smith, W.H.F. & Wessel P., 1990. Gridding with continuous curvature splines in tension, *Geophysics*, **55**, 293-305.

Thompson, D.A., Bastow, A.D., Helffrich, G., Kendall, J.-M., Wookey, J., Snyder, D.B., & Eaton, D.W., 2010. Precambrian crustal evolution: Seismic constraints from the Canadian Shield, *Earth Planet. Sci. Lett.*, **297**, 655-666

Tkalčić, H., Rawlinson, N., Arroucau, P., Kumar, A. & Kennett B.L.N., 2012. Multi-step modelling of receiver-based seismic and ambient noise data from WOMBAT array: crustal structure beneath southeast Australia, *Geophys. J. Int.*, **188**, 1681–1700.

an der Beek, P., Braun, J. and Lambeck, K., 1999. Post-Palaeozoic uplift history of southeastern Australia revisited: results from a process-based model of landscape evolution. *Austral. J. Earth Sci.*, **46**, 157–172.

van der Hilst, R., Kennett, B.L.N., Christie, D., & Grant, J., 1994. Project SKIPPY explores the lithosphere and mantle beneath Australia, *EOS Trans. AGU*, **75**, 177

Wessel, P. & Smith, W.H.F., 1998. New, improved version of generic mapping tools released, *EOS, Trans. Am. Geophys. Un.*, **79**, 579.

Young, M.K., Rawlinson, N., Arroucau, P., Reading, A.M., & Tkalčić, H., 2011. High-frequency ambient noise tomography of southeast Australia: New constraints on Tasmania's tectonic past, *Geophys. Res. Lett.*, **38**, L133313, doi:10.1029/2011GL047971.

APPENDIX A: DENSITY DISTRIBUTION

The density distribution derived from the AuSREM P wavespeed results is illustrated in Figure A1 at 5 km intervals from 5 to 30 km depth. the first impression is that there is little density variation, but in fact there are significant gradients at all depths. The nature of the available constraints means that that prominent features in the gravity field, such as the major east-west anomalies in Central Australia are not represented in detail. However, we hope that the density field for the AuSREM crust can provide a starting point for more localised studies.

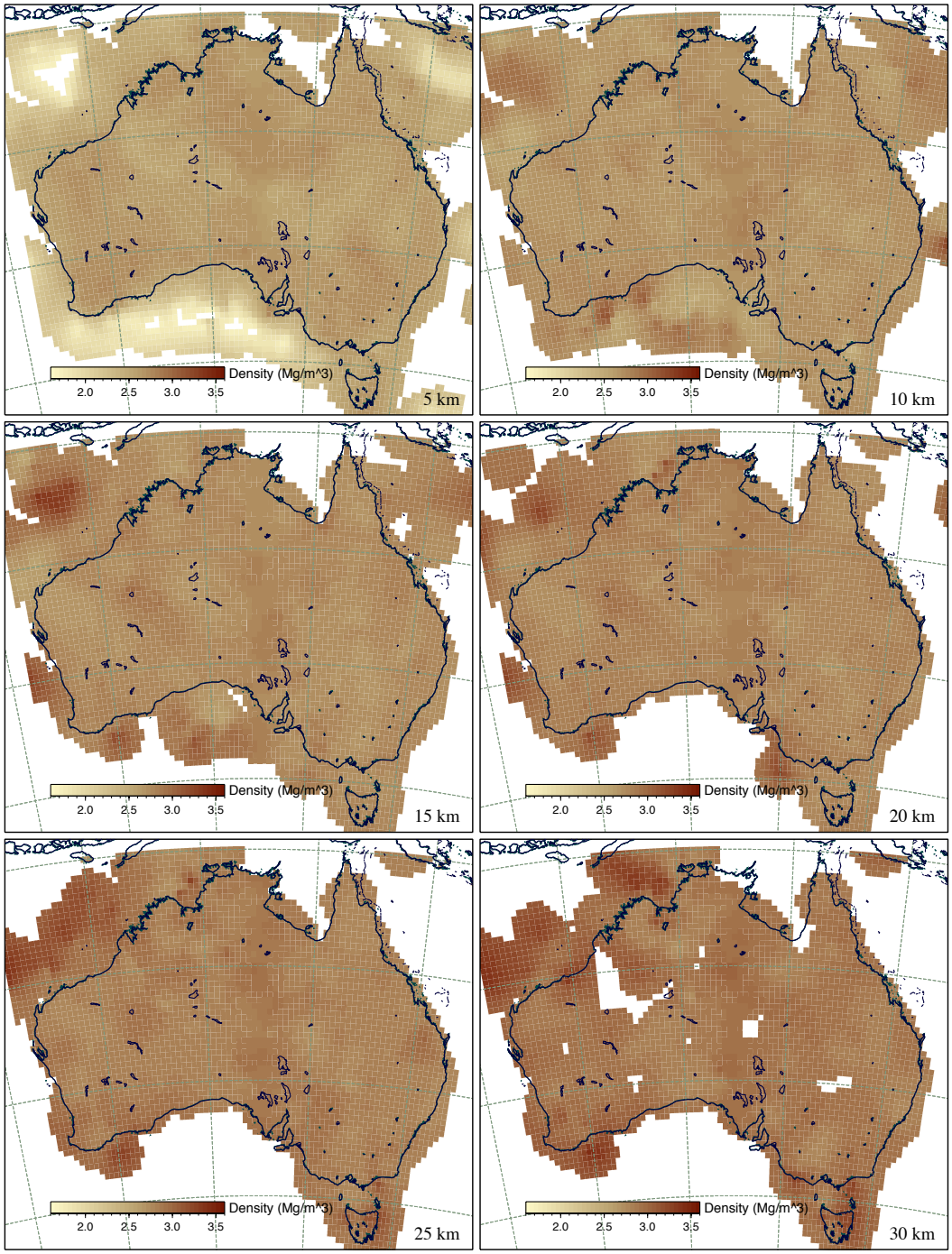

Figure A1. Distribution of density (ρ) for the AuSREM crustal model at: (a) 5 km depth, (b) 10 km depth (c) 15 km depth, (d) 20 km depth, (e) 25 km depth, (f) 30 km depth.